Research Square

Preprints are preliminary reports that have not undergone peer review.
They should not be considered conclusive, used to inform clinical practice,
or referenced by the media as validated information.

Measurement and Regulation of Residual Stress in Door Opening Welds of Wind Turbine Towers

Liu Hui
liao ning gong cheng ji shu da xue: Liaoning Technical University
Sun Wanting
wt230416@163.com
liao ning gong cheng ji shu da xue: Liaoning Technical University https://orcid.org/0009-0004-9434-6172
Zhong Zhenqian
liao ning gong cheng ji shu da xue: Liaoning Technical University
Li Pengfei
liao ning gong cheng ji shu da xue: Liaoning Technical University

Research Article

Keywords: Wind turbine tower, residual stress, ultrasonic impact treatment, heat treatment, X-ray diffraction, fatigue performance

Posted Date: May 21st, 2026

DOI: https://doi.org/10.21203/rs.3.rs-9546590/v1

License: This work is licensed under a Creative Commons Attribution 4.0 International License.
Read Full License

Abstract

Weld residual stress is a critical factor affecting the structural integrity and service life of wind turbine towers. In this study, a systematic investigation was conducted on the residual stress distribution and control methods for door corner welds of an in-service wind turbine tower after approximately 20,000 hours of operation. X-ray diffraction (XRD) measurements revealed significant tensile residual stress in the weld and heat-affected zone, with peak values reaching 315 MPa, particularly concentrated at depths of 5–7 cm. To mitigate these stresses, two post-weld treatment methods were employed: ultrasonic impact treatment (UIT) and localized heat treatment. UIT effectively transformed surface tensile stress into compressive stress, achieving a maximum compressive residual stress of -400 MPa within a depth of 3 cm, while simultaneously refining grains and increasing surface hardness. In contrast, localized heat treatment at 460°C for 5 hours led to a broader stress relief effect, reducing residual stress by approximately 100 MPa without causing significant changes to the macrostructure, but inducing substructural rearrangements beneficial for stress relaxation. The results of the mechanical performance tests indicate that both regulation processes improved the strength, plasticity, and toughness of the welds. The combined findings demonstrate that ultrasonic impact treatment is highly effective for enhancing fatigue performance at the surface, while localized heat treatment offers advantages for deep stress redistribution and long-term structural stability. This study provides an important technical reference and experimental basis for the regulation of residual stress in complex welded structures of wind turbine towers, and possesses significant engineering application value and prospects for wider adoption.

1. Introduction

Welding residual stress is a key factor affecting the safety and service life of wind tower structures, especially in the welds of Door Opening corner Welds area, as shown in Fig. 1. Complex welded regions such as door opening corner welds are prone to high residual tensile stresses, which can lead to delayed cracking, fatigue failure, and other issues, thus posing a threat to the stability of the tower. Given this characteristic of wind towers, conducting systematic testing and control studies of residual stress is particularly important. Hobbacher et al.[1, 2] proposed a high-precision residual stress testing method, focusing on analyzing the weld characteristics in door opening corner welds area, providing a theoretical foundation for subsequent research on testing and control technologies. This study experimentally verified the spatial distribution and stress gradient of welding residual stress, enhancing the understanding of complex welded regions.

In terms of residual stress testing methods, various high-precision non-destructive testing techniques, such as X-ray diffraction (XRD), synchrotron radiation, and neutron diffraction, have been widely adopted internationally. Pérez et al.[3–5] explored the application of X-ray diffraction technology in detecting residual stress in welded areas, further verifying its applicability in wind tower structures. Although X-ray diffraction technology is well-established in the application of thin-walled materials, its application in thick-walled structures still faces certain challenges, such as high requirements for the sample surface

condition and the inability to effectively penetrate thicker materials. Schajer et al.[6–8] used synchrotron radiation to study the variation of residual stress in welded joints and proposed the advantages of this technology in high-precision stress testing. However, despite the strong material penetration ability of synchrotron radiation, the high equipment costs and operational complexity limit its application in practical engineering. To address this issue, Yang et al.[9–11] proposed field application techniques based on ultrasonic testing and the blind hole method, which facilitate real-time monitoring in field inspections of larger structural components. Although these methods have high practicality, they still struggle to provide the same accuracy as high-precision methods, especially when measuring deep residual stress.

In the control of residual stress, research mainly focuses on methods such as mechanical processing, heat treatment, and emerging vibration stress relief (VSR) technology. He et al.[12–14] studied laser shock peening technology, proposing the induction of deep residual compressive stress through a non-contact method, which has been widely applied in aerospace and wind power fields. Laser shock peening can effectively improve the fatigue strength of materials and induce deep residual compressive stress, but its high cost and poor adaptability to complex-shaped components may limit its application, especially in large welded components of wind tower structures. Additionally, Liu et al.[15–17] also verified the effectiveness of ultrasonic impact treatment in controlling residual stress in welded areas. The results showed that ultrasonic impact treatment significantly reduced tensile stress in the weld region, thereby improving fatigue life. However, although ultrasonic impact technology offers advantages such as ease of operation and low cost, its control effect on high-stress concentration areas remains limited, and the results vary in welded joints of different materials and thicknesses.[18, 19] Therefore, achieving customized control for different welded joints in field environments remains an important issue in current research.

Despite significant progress in the above testing and control technologies, systematic testing and control of residual stress still face certain technical gaps in the complex field environment of wind tower structures, especially in high-stress concentration areas.[20–23]For example, the applicability of existing testing methods in different materials, thicknesses, and complex structures remains limited, making it difficult to achieve large-scale, real-time stress monitoring.[24–29] As for the current control technologies, such as laser shock peening and ultrasonic impact treatment, while they can improve the residual stress state in welded areas to some extent, their effectiveness in controlling deep residual stress is limited, and their stability and effectiveness in some special environments have not been fully verified.[30–34] To meet the growing demand for larger capacity and longer service life of wind power equipment, conducting in-depth research on the residual stress in door opening corner welds area is of great engineering significance and practical value.[35–38] By different testing methods and control technologies, the safety and service life of wind tower structures can be effectively improved, providing technical support for the sustainable development of the wind power industry.[39, 40]

2. Methods

In order to obtain the residual stress distribution at different depths of door opening corner welds surface(Model: 6.25 MW wind turbine), this study uses the layer-by-layer peeling method in conjunction with an X-ray diffraction device (Model: X-RAY Stress Analyzer) for measurement, as X-ray testing only measures planar stress. Controlled-depth corrosion was performed on the specimen surface using an electrolytic polishing machine (Model: EP-5010), with approximately 0.5 cm of material removed during each step. After each layer was removed, residual stress measurements were conducted on the newly exposed surface using the X-ray diffraction method. By repeating this process and progressively removing material to the predetermined depth, the residual stress distribution as a function of depth was obtained.

In this study, residual stress in the door opening welds of wind turbine towers was regulated using a combined approach of ultrasonic impact treatment (Model: UIT-200) and local heat treatment (Model: LWK-I-60KW). The microstructural changes in the welds after both treatments were thoroughly examined using a metallographic microscope (Model: VERTAI3848000710). The mechanical properties of the treated specimens were evaluated using a tensile testing machine (Model: ZWICK-Z1200), and hardness variations before and after treatment were measured with a Vickers hardness tester (Model: KB-30-SR-FA). The effectiveness of the two regulation methods in optimizing the residual stress distribution and their associated microstructural evolution were systematically analyzed. By performing stress regulation and measurement simultaneously, the effects of different control parameters were compared to determine the most suitable residual stress regulation method and key process parameters for the door opening welds of wind turbine towers.

3. Residual Stress Measurement

3.1 Specimen Preparation

Figure 2 shows the test sample, which was extracted from door opening corner welds area (material: Q355). Two base metals were welded to form a corner weld. The welding protective gas used was CO_2, and the welding wire (ER50-6) had a specification of 0.12 cm. Subsequently, electrolytic polishing was performed to a depth of 0.5 cm to obtain a smooth, defect-free surface, ensuring reliable diffraction signals for accurate residual stress measurements.

3.2 X-Ray Stress Analyzer Parameter Settings

The residual stress measurements were conducted using an X-ray stress analyzer. The detailed parameter settings are as follows: The crystal structure was body-centered cubic (BCC), and the diffraction plane was [41]. A Cr-Kα radiation source was used. The X-ray elastic constants were $\frac{1}{2}\int_{2}^{\{hkl\}} dx$=5.81×10-6mm2N-1; $\int_{1}^{\{hkl\}} dx$=-1.27×10-6mm2N-1.The stress measurement was performed using the sin²ψ method, and the peak positions were determined by the fitting method. The tube current and voltage were set to 1.03 mA and 19.78 kV, respectively. A collimator with a diameter of 2 mm was used, and the data acquisition time for each measurement was 40 seconds.

3.3 Residual Stress Distribution at Various Depths

In this study, three measurement points (test1, test2, and test3) were selected, as illustrated in Fig. 3(a), and the corresponding stress-depth distribution curves were obtained, as shown in Fig. 3(b). As shown in the figure, residual stresses at all measurement points remained in a tensile state within the 0 ~ 10 cm depth range, indicating a significant accumulation of welding-induced residual tensile stress in the weld region. Among the three, test1 exhibited the highest stress peak, reaching approximately 315 MPa, which was notably higher than those at the other two measurement points, suggesting the presence of a local stress concentration in this area. Along the depth direction, the residual stress demonstrated a general trend of initially increasing and then gradually decreasing, with pronounced stress peaks observed at depths of approximately 5 cm and 7 cm. This pattern was consistently observed across all three measurement curves, indicating its representativeness. Therefore, the 5 ~ 7 cm depth range can be identified as a critical region for stress regulation, which should be specifically targeted for treatment and monitoring during subsequent control procedures to effectively lower the residual tensile stress peaks, enhance the mechanical performance of the weld, and prevent the initiation and propagation of delayed cracking.

4. Regulation of Residual Stress by Ultrasonic Impact Treatment and Local Heat Treatment

4.1 Ultrasonic Impact Treatment

4.1.1 Specimen Preparation and Ultrasonic Impact Machine Parameter Settings

The ultrasonic impact treatment was carried out using the specimens tested for residual stress in Section 3.1, and the areas not subjected to electrolytic corrosion in Section 3.1 were selected for the impact operation. This specimen selection approach allows for a direct comparison of residual stress data before and after ultrasonic impact treatment, providing a more intuitive and effective evaluation of the treatment’s effectiveness and applicability in residual stress regulation.

The door opening welds of the wind turbine tower were treated using an ultrasonic impact machine (Model: UIT-200). The ultrasonic impact treatment was performed at a frequency of 27 kHz, with an amplitude of 25 μm and an applied pressure of approximately 20 N. A multi-pin impact tool was employed to uniformly process the weld and heat-affected zone, with the feed rate maintained at 20 mm/s. An impact duration of approximately 15 seconds was applied at each treatment point to ensure stable and uniform stress regulation.

4.1.2 Residual Stress Results After Ultrasonic Impact Treatment

In this test, three different test points (test1, test2, test3) were selected on the impacted sample, and three points (test4, test5, test6) were selected at non-impacted locations. The comparison curves of residual stress versus measurement depth are shown in Fig. 4. As seen from the figure, after ultrasonic impact treatment, the weld surface region exhibits a distinct residual compressive stress state. The maximum compressive stress value occurs at the surface layer, approximately − 372 MPa, indicating that ultrasonic impact has induced a strong compressive stress field on the material surface. The three stress-depth curves exhibited highly consistent trends with good repeatability and representativeness, confirming the stability and reliability of the stress regulation achieved through the treatment.

From the perspective of depth variation trends, the stress gradually transitions toward the neutral axis as the depth increases. Compressive stress gradually weakens and transitions to tensile stress at approximately 3 cm, indicating that the influence range of compressive stress is about 3 cm, and the residual stress decreases by up to approximately 600 MPa. Compared to the untreated condition, ultrasonic impact treatment significantly reduced the surface tensile stress and generated a compressive stress layer within a certain depth range, thereby effectively regulating the residual stress in the weld. Based on the analysis of the stress distribution characteristics, the 0 ~ 3 cm depth range can be identified as the primary compressive stress zone, further confirming that the effective regulation depth of ultrasonic impact treatment is approximately 3 cm.

4.2 Local Heat Treatment

4.2.1 Heat Treatment Furnace Parameter Settings

The heat treatment process parameters were set as follows: 200°C for 3 hours, 200°C for 50 hours, 350°C for 50 hours, and 460°C for 5 hours.

4.2.2 Residual Stress Results After Heat Treatment at Different Temperatures

Figure 5:(a); (b) shows the residual stress distribution under different heat treatment temperatures and holding times. Compared to the untreated samples in Section 3.3, the heat treatment conditions of 200°C for 3 hours, 200°C for 50 hours, and 350°C for 50 hours had little effect on performance, as the parent material consisted of normalized ferrite and pearlite microstructure, and tempering below 460°C had minimal impact. However, under the condition of 460°C for 5 hours, residual stress was significantly controlled. The overall stress level decreased, with a control range of about 100 MPa. Notably, at depths of 5 cm and 7 cm in the weld, the residual stress peak was significantly reduced. It indicates that this heat treatment condition has a more significant effect on optimizing welding residual stress compared to the ultrasonic impact method.

5. Experimental Verification of Residual Stress Regulation Effectiveness

5.1 Microstructural Analysis

Figures 6(a)-(d) show the microstructure of the weld surface and internal plastic deformation layer formed after ultrasonic impact treatment. As seen in Fig. 6(b), the weld microstructure consists of blocky acicular ferrite + bainite. After ultrasonic impact, the microstructure exhibits a deformed streamline distribution, perpendicular to the direction of impact. According to the image, there is an obvious deformed layer, which is consistent with the regulation through residual stress testing in Section 4.1.2. A significant change in the microstructure can be observed by comparing Fig. 6(c) and Fig. 6(d) in different areas. In the undeformed region, the grains are relatively large, with a columnar or irregular shape, loosely arranged, and the grain boundaries are clearly visible. In contrast, at the surface (Fig. 6(b)) and in the deformed region (Fig. 6(bd)), the grains are significantly refined, the spacing between them is reduced, and the microstructure tends to become denser, with grain size refined from 100 μm to below 20 μm. These changes indicate that significant plastic deformation and grain redistribution occurred in the material under ultrasonic impact loading.

Figure 6(e) and (f) shows the microstructure before and after heat treatment, respectively. It is observed that the microstructure remains as blocky acicular ferrite + bainite both before and after heat treatment. The macro-grain morphology of the material remains largely consistent, with no significant grain growth or recrystallization, indicating that localized heat treatment did not significantly affect the overall microstructure. However, at the microscopic scale, rearrangement and subtle changes within the substructure of the grains are observable, reflecting that the material underwent a recovery process. This substructure adjustment helps release the residual stresses introduced during the processing, enabling effective stress control without damaging the stability of the original grain morphology.

5.2 Hardness Analysis

As shown in Fig. 7, Vickers hardness testing was conducted on untreated samples, ultrasonic impact samples, and locally heat-treated samples. The testing used the metallographic specimens described in Section 5.1. As shown in Fig. 7(a), the hardness measurements were conducted in a zigzag pattern under a test load of 300 g, the holding time was 15 s.

Figure 7(b) presents the hardness profiles before and after ultrasonic impact treatment. The comparison demonstrates a significant increase in surface hardness following ultrasonic impact, with the maximum hardness reaching 333 HV, indicating substantial plastic deformation. As the testing depth increased, the hardness gradually decreased, exhibiting a transition from the plastically deformed surface layer to the undeformed base material. Beyond a depth of approximately 3 cm, the hardness stabilized at around 216 HV, suggesting that this region corresponded to the original substrate and was no longer affected by the ultrasonic impact treatment.

Figure 7(c) presents the hardness curves obtained before and after heat treatment. The comparison shows that local heat treatment reduced the material hardness by 60 HV. This observation suggests

significant substructure rearrangement and a decrease in dislocation density occurred during heat treatment, which would be expected to weaken the work hardening effect. Such softening behavior is considered to be closely related to residual stress relief. As the dislocation network is eliminated and lattice internal stresses are relaxed, the internal stress field tends to become more uniform, which presumably contributes to the effective reduction in residual stress.

5.3 Mechanical Properties Evaluation

Tensile specimens (Φ5 cm) and V-notch impact specimens (10 cm × 10 cm × 55 cm) were prepared from the welds after local heat treatment, and room temperature tensile and impact tests were conducted. As shown in Table 1, after heat treatment, the weld specimens exhibited excellent strength, ductility, and toughness, significantly exceeding the minimum specification requirements. The tensile strength remained consistently above 540 MPa, while both elongation and reduction of area values maintained high values. In addition, a significant improvement in impact energy was observed.

Table 1
Tensile and Impact Test Results

Specimen Type	Tensile Strength(MPa)	Yield Strength(MPa)	Elongation (%)	Reduction of Area (%)	Impact Energy (J)
Weld 1	543	424	21.5	70	64, 78
Weld 2	544	428	23	67	36, 81
Specification Requirement	470–630	≥ 355	≥ 20	/	/

6. Conclusion

In this study, a systematic investigation was conducted on the residual stress issues present in the door opening welds of wind turbine towers, focusing on both measurement and regulation. residual stress measurements using X-ray diffraction revealed high residual tensile stresses in door opening corner welds, with the maximum stress reaching 315 MPa. Significant stress concentrations were identified at depths of 5 cm and 7 cm within the weld, which may serve as potential initiation sites for fatigue damage.

For residual stress regulation, two typical process routes -- ultrasonic impact treatment and local heat treatment -- were employed in this study. The regulation effects were systematically evaluated through metallographic analysis, mechanical property testing, and hardness distribution measurements. Ultrasonic impact treatment induced significant plastic deformation in the surface layer, effectively converting residual tensile stress into residual compressive stress within a depth of 3 cm, with a maximum regulation amplitude of 600 MPa. In addition, this method resulted in pronounced grain refinement, microstructural densification, and surface hardness enhancement, thereby effectively

improving the fatigue resistance of the weld surface. Under the conditions of local heat treatment at 460°C for 5 hours, deeper stress relief and redistribution are achieved, exhibiting good stress homogenization capability, while exerting a relatively mild impact on the overall microstructure and mechanical properties of the material, demonstrating deep and wide-ranging regulatory advantages.

Comprehensive analysis indicates that ultrasonic impact treatment is highly effective in enhancing the fatigue performance of the weld surface and delaying crack initiation and propagation, making it well-suited for surface strengthening in fatigue-sensitive areas. In contrast, local heat treatment is more appropriate for overall stress optimization in macrostructures and for improving long-term service reliability. Each regulation method has distinct advantages in terms of application scope and underlying mechanisms, thereby complementing each other effectively. The findings of this study provide reliable experimental evidence and technical guidance for multi-scale and hierarchical residual stress regulation in complex welded structures such as door opening welds of wind turbine towers, offering considerable engineering significance and promising application prospects.

Declarations

Acknowledgments: There are no additional contributors to acknowledge beyond the listed authors.

Author contributions: Hui Liu: Methodology, Project administration, Supervision, Writing - review and editing. *Wanting Sun: Writing - original draft, Data curation, Visualization. Zhenqian Zhong: Conceptualization, Supervision, Validation. Hongyue Chen: Methodology, Supervision. Jianglin Lan: Investigation. Rui Zhao: Investigation.

Conflicts of interest or competing interests: The authors declare no competing interests.

Data and code availability: Not applicable. This study involved the following authors:Hui Liu, *Wanting Sun ,Zhenqian Zhong,Hongyue Chen,Jianglin Lan,Rui Zhao

Supplementary information: Not applicable.

Ethical approval: Not applicable.

References

1. MeixiaWang et al Advances in experimental measurement methods of residual stress in laser cladding layer %J. Int J Adv Manuf Technol. 2026(prepublish): p. 1–30
2. Ashikari Y et al (2026) Development of a thin-film residual-stress measurement device using multi-folded structures %J. Jpn J Appl Phys. 65(6): p. 06SP20-06SP20.
3. Armitage L et al (2026) The use of residual lower limb –prosthetic socket interface pressure measurements to inform clinical decisions: A systematic review %J. J Biomech 199:113187–113187

4. Luo Z et al (2026) (prepublish) Correction: Optimization of Finite Element Mesh for Residual Stress Measurement Using Contour Method %J Experimental Techniques. : pp. 1–3
5. DebRoy T et al (2026) Residual stress and distortion in fusion welding and fusion-based additive manufacturing: measurements, mechanisms and control strategies %J. Prog Mater Sci 159:101651–101651
6. Hatos I (2025) Improvement of the cantilever test geometry deflection measurement method to assess residual stresses in laser powder bed fusion %J. Prod Eng Archives 31(4):474–480
7. Mansourian R, Mahmoodi M (2025) Measurement of residual stress due to deformation caused by slight hydroforming deformation process in double-walled pipes through external pressure %J. J Adv Join Processes 12:100338–100338
8. Szabó V, Hatos I, Weltsch Z (2025) Understanding and analyzing the effect of residual stresses in direct metal laser sintering through optical deformation measurement %J Progress in Additive Manufacturing. 11(1):1–13
9. Kleiman J, Smilenko V, Kot V Accounting for temperature influence in non-destructive measurements of applied and residual stresses by ultrasonic method %J Welding in the World. 2025(prepublish): pp. 1–14
10. Mitsui S et al (2026) X-ray residual stress measurement under non-ideal conditions using silicon-on-insulator pixel detectors %J Nuclear Inst. and Methods in Physics Research, A. 1081:170856–170856
11. Qi Q et al (2025) Measurement of residual stresses in slender support plates in aeroengine inlet case based on the sampling Moiré method %J Measurement. 253(PD):117781–117781
12. Jimenez I et al (2025) Measurement of Residual Stress in 316L Produced by Laser-Based Powder Bed Fusion %J. J Mater Eng Perform 34(20):1–14
13. Alkaisee R, Karlsson H (2025) Material Examinations and Residual Stress Measurements of Additively Manufactured Steel Components %J. J Mater Eng Perform 34(10):1–9
14. Wilvert T, Viotti MR, Jr AA (2025) Numerical evaluation of iterative algorithm for plasticity effect correction in residual stress measurements using radial DSPI and the hole-drilling method %J. Opt Lasers Eng 186:108790–108790
15. Huang X et al (2026) Rapidly regulating dislocations in dual-phase brass through pulsed electric current to weaken high-value residual stresses %J. J Mater Res Technol 42:1736–1748
16. Yang X et al (2026) Microstructural evolution governing magnetostriction in additively manufactured Fe81Ga19 alloys during annealing: The interplay of texture, L60 nanoprecipitates, and residual stress %J. J Alloys Compd 1059:187139–187139
17. Yang Z et al (2026) Temperature-governed lattice disorder, residual stress, and recovery in CVD 4H-SiC under Al implantation and annealing %J. J Alloys Compd 1054:186279–186279
18. Liu G et al (2025) Revealing the passivator orientation on defect healing and residual strain regulation in all-inorganic perovskite solar cells %J. Chem Eng J 522:167395–167395

19. Kai G, Wenjie L (2024) Improving mechanical properties of additively manufactured H13 steel through residual stress modulation by laser shock peening %J. Int J Adv Manuf Technol 132(11–12):5289–5303
20. Jiazheng H et al (2023) Residual stress measurement system of the general purpose powder diffractometer at CSNS %J Nuclear Inst. and Methods in Physics Research, A. 1055
21. Patrik Š, Štefan B, František T (2017) Design of a Bend Testing Machine for Determination of Residual Stresses by the MTS-3000 Ring-Core System %J. Am J Mech Eng 5(6):269–273
22. Qi L, Siyu J, Bin S (2023) Precisely tuning the residual stress anisotropy in machine hammer peening %J. Int J Adv Manuf Technol 127(9–10):4577–4589
23. Zhenyu C et al (2023) Ductility enhancement of additively manufactured CoCrMo alloy via residual stress tailored high stacking fault probability %J. Scripta Mater. 235
24. Qin R et al (2025) Explainable deep learning framework for residual stress monitoring in laser shock peening via acoustic emission %J. J Industrial Inform Integr 47:100904–100904
25. V., M.e.V., T.K. A., and L.k.S. V., On the Question of Monitoring Residual Stresses in Selectively Heat-Strengthened Rails %J. Russ J Nondestr Test. (2018) 54(10): p. 675–681
26. Koki I, Ken S, Hideo M (2017) Development of a Residual Stress Monitoring Sensor for Electronic Devices %J The Proceedings of Mechanical Engineering Congress, Japan. 2017(0): pp. J0330202-J0330202
27. Pouria K et al (2024) In situ measurements and simulation of residual stresses and deformations in additively manufactured thin plates %J. Int J Adv Manuf Technol 132(7–8):4055–4068
28. Beghini M et al (2024) Regularization of Hole-Drilling Residual Stress Measurements with Eccentric Holes: An Approach with Influence Functions %J. J Mater Eng Perform 33(15):7652–7658
29. Suk HC, Soon PS, Gyu CM (2024) Investigation of the characteristics of TiN-coating film deposited by arc ion plating method and the feasibility of measuring residual stress according to heat treatment %J. J Korean Phys Soc 84(10):779–792
30. Alloys, Findings from Beihang University Has Provided New Data on Alloys and (2018) Compounds (Microstructure, residual stress and tensile properties control of wire-arc additive manufactured 2319 aluminum alloy with laser shock peening) %J. Chemicals & Chemistry
31. Song T et al (2013) W.,., Regulation of residual stress in elastic solid component with high-energy acoustic field %J AIP Conference Proceedings. 1511(1): p. 1196
32. Hua S et al (2011) Straightening Regulation Optimization on the Residual Stress Induced by the Compound Roll Straightening in the Heavy Rail %J Shock and Vibration. 18:171–180
33. D. OM (2024) Near Edge Residual Stress Measurement Using Incremental Hole Drilling %J Experimental Mechanics. 64(4):501–517
34. Mousa SM, Hameed AS, Ibrahim AF (2024) Measurement from the residual stresses on magnetic abrasive finishing process by utilizing steel sheet 201%J Multiscale and Multidisciplinary Modeling, Experiments and Design. 7(3):2605–2614

35. Schoderböck P, Ploner K (2026) Material machining-induced near-surface residual stress states: An X-ray diffraction and electron-microscopy study on a tungsten plate %J. Int J Refract Met Hard Mater 136:107587–107587
36. Shiyu Q, Jun T, Yifan W (2025) Relationship between residual stress and fatigue performance of TC4 alloy components with different surface states %J Journal of Physics: Conference Series. 3093(1): pp. 012002–012002
37. Khodabakhshi F et al (2019) Tailoring the residual stress during two-step cold gas spraying and friction-stir surface integration of titanium coating %J. Surf Coat Technol 380:125008–125008
38. Science - Mechanical Science; Huazhong University of Science and Technology Reports Findings in Mechanical Science (2018) Adjustment of machining-induced residual stress based on parameter inversion) %J. Journal of Technology & Science
39. Popiela B et al (2025) Impact of internal pressure control during manufacturing on residual stresses and safety performance of type 4 pressure vessels %J Composites Part C. Open Access 17:100581–100581
40. □□□ et al (2014) Three Dimensional Wrinkling at Metal/Polymer Interfaces by Residual Stress Manipulation %J
41. Yu Y et al (2026) Coupling of diffusion-induced and thermal stresses in solid-state lithium-ion batteries: A fully 3D electrochemical-thermal-mechanical model %J Case Studies in Thermal Engineering. 81:107979–107979

Figures

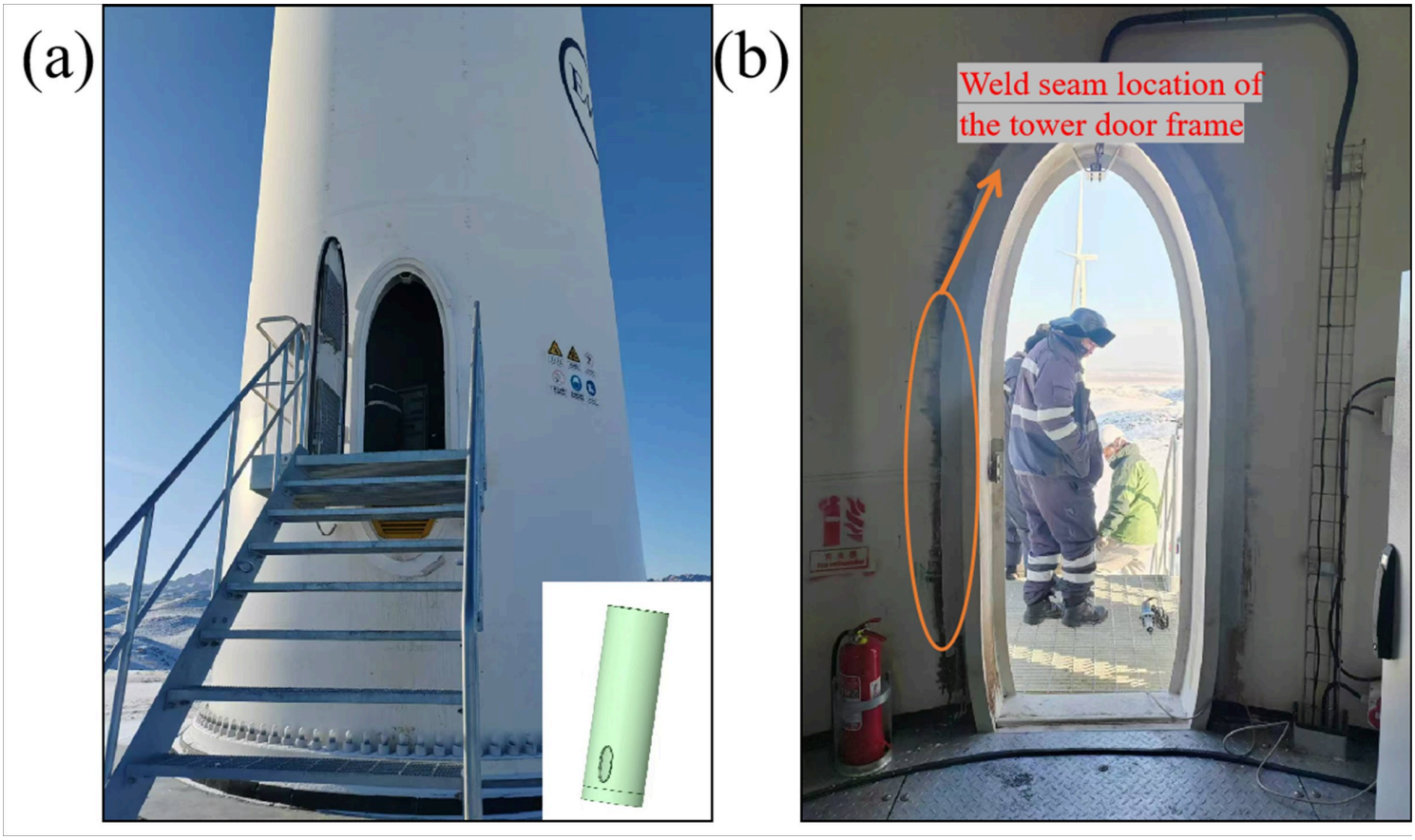


Figure 1

Weld location of door opening corner welds: (a) Door opening position on the wind turbine tower ; (b) Corner welds location of the door opening

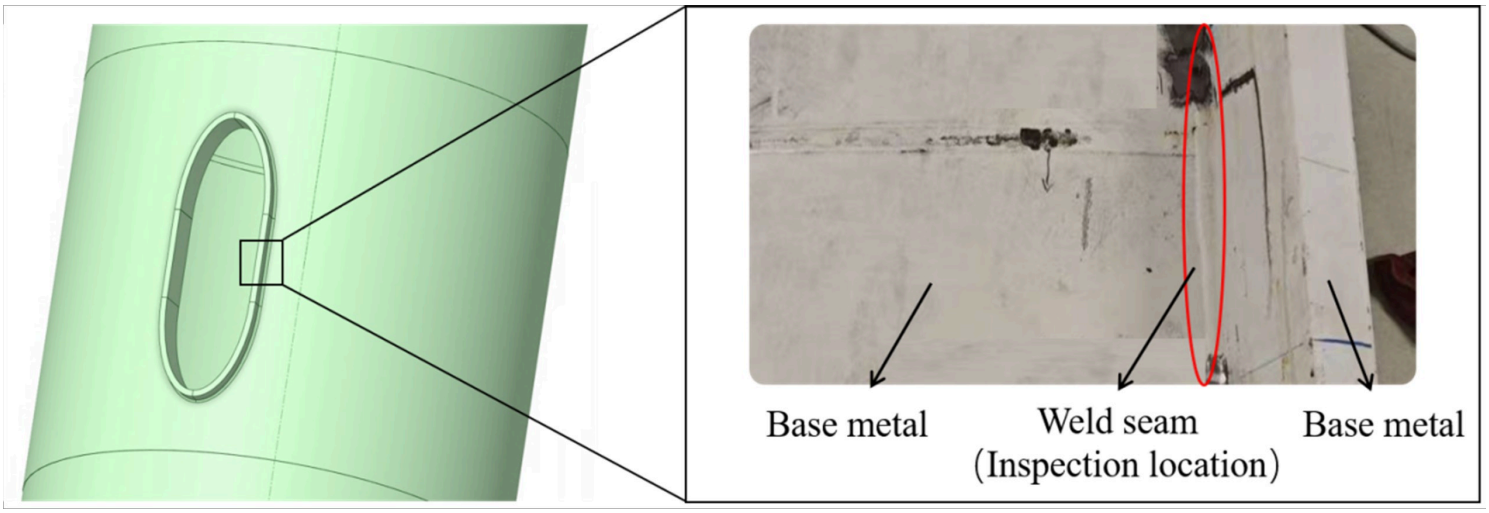


Figure 2

Weld seam testing location of door opening corner welds: (a) Sample collection location; (b) Test Sample

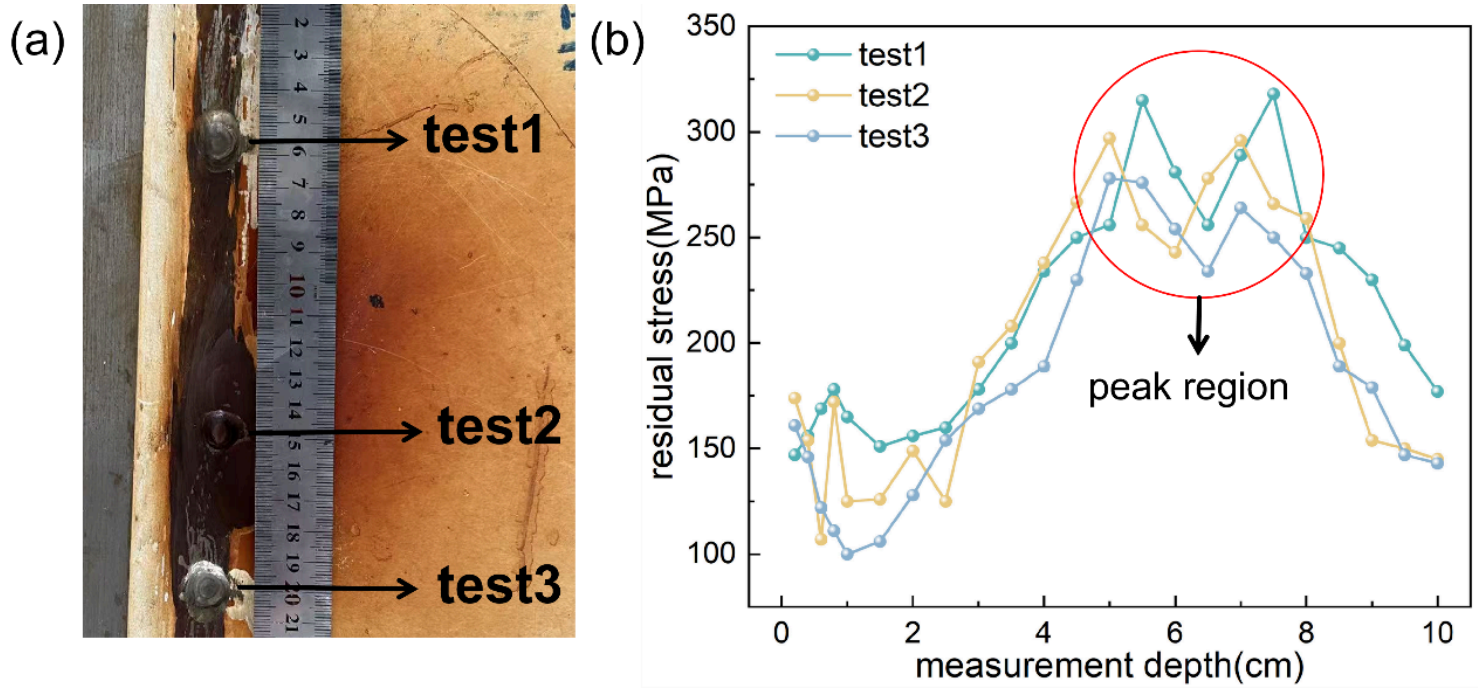


Figure 3

Residual stress measurement results prior to treatment: (a) Measured locations; (b) Residual stress values with different depths

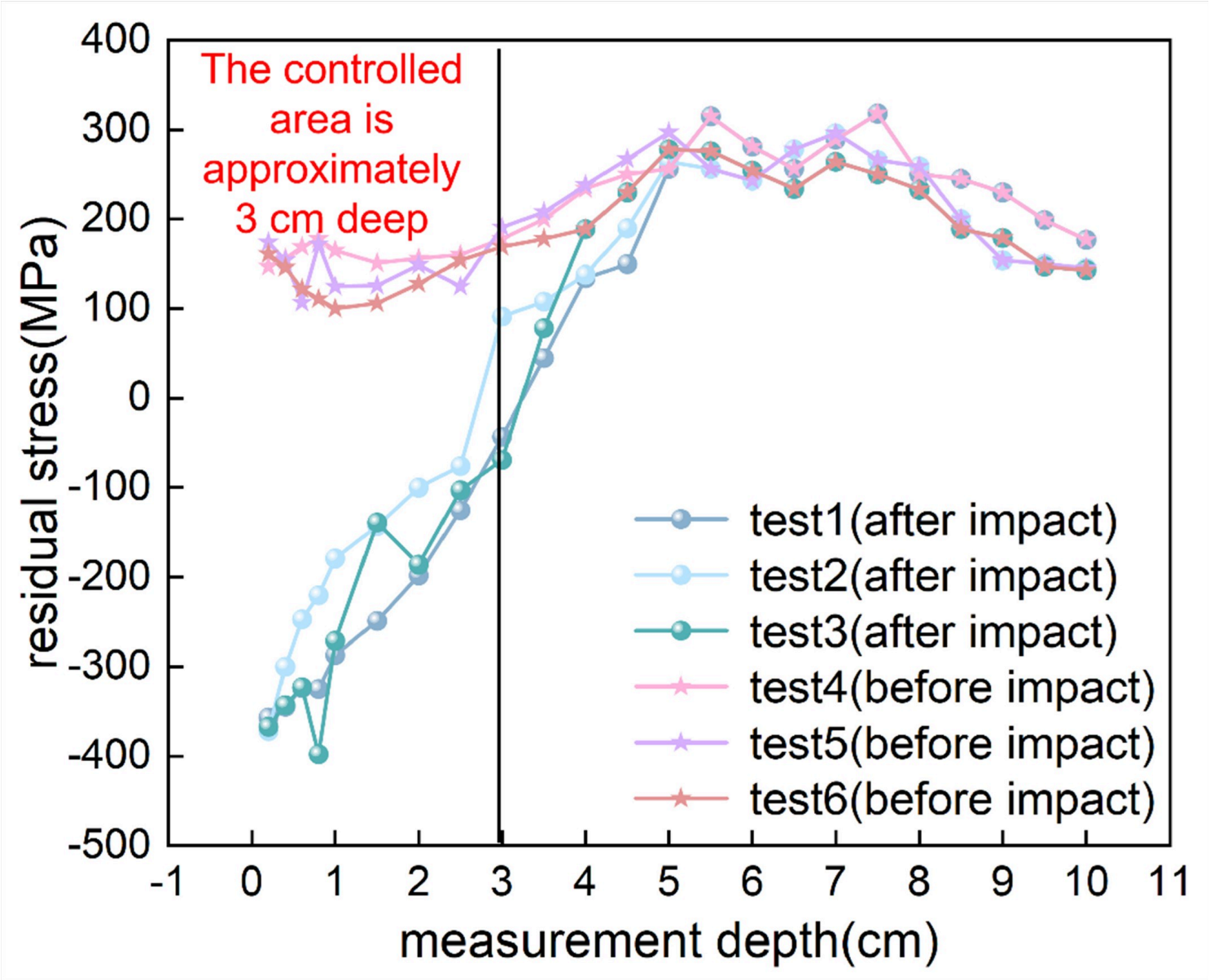


Figure 4

Comparison Chart of Residual Stress Before and After Ultrasonic Impact

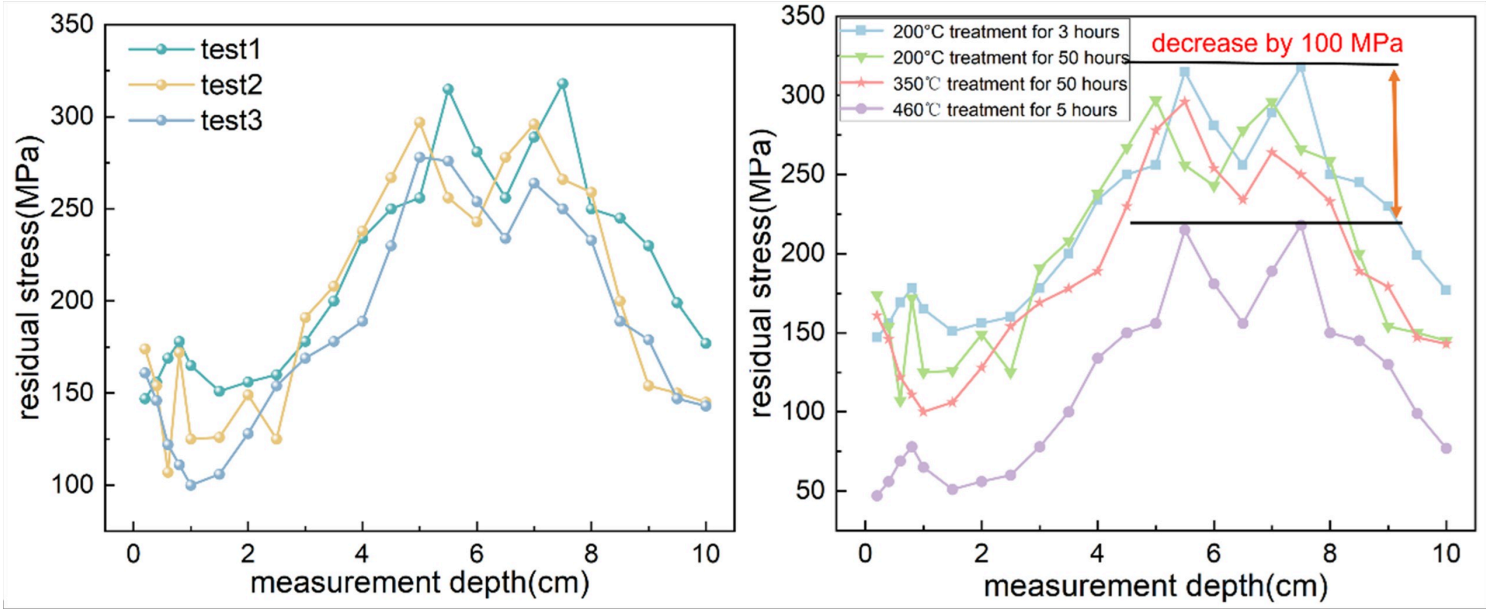


Figure 5

Test results after heat treatments at various temperatures:(a) Section 3 Results of Residual Stress Before Regulation;(b) Residual Stress Results After Heat Treatment

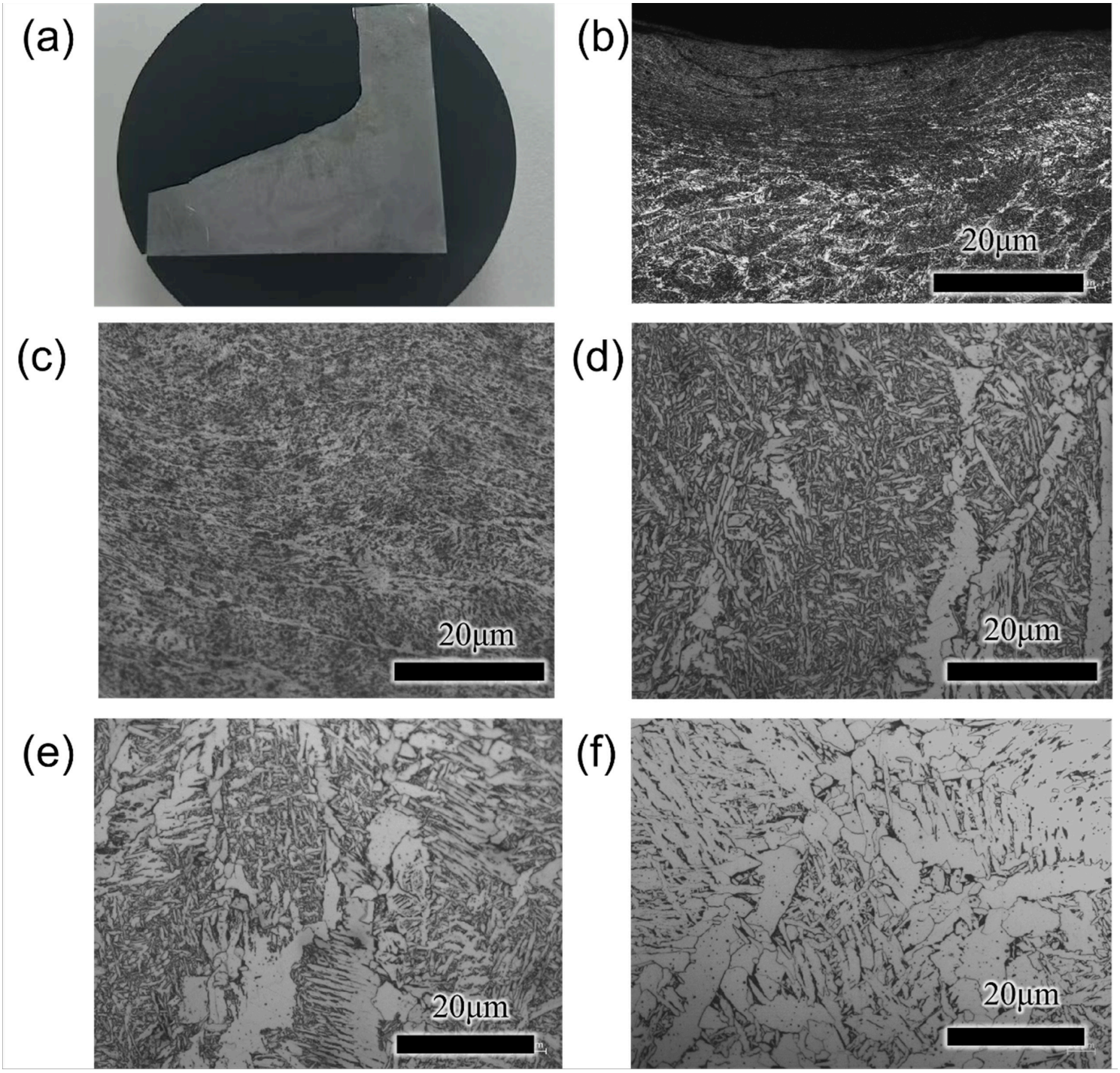


Figure 6

Microstructural changes before and after ultrasonic impact treatment or heat treatment: (a) Weld subjected to ultrasonic impact; (b) Enlarged microstructure of (a)--around the surface; (c) Enlarged microstructure of (a)--undeformed erea; (d)Enlarged microstructure of (a)--ultrasonically impacted deformed erea; (e) Metallographic structure before heat treatment; (f) Metallographic structure after heat treatment

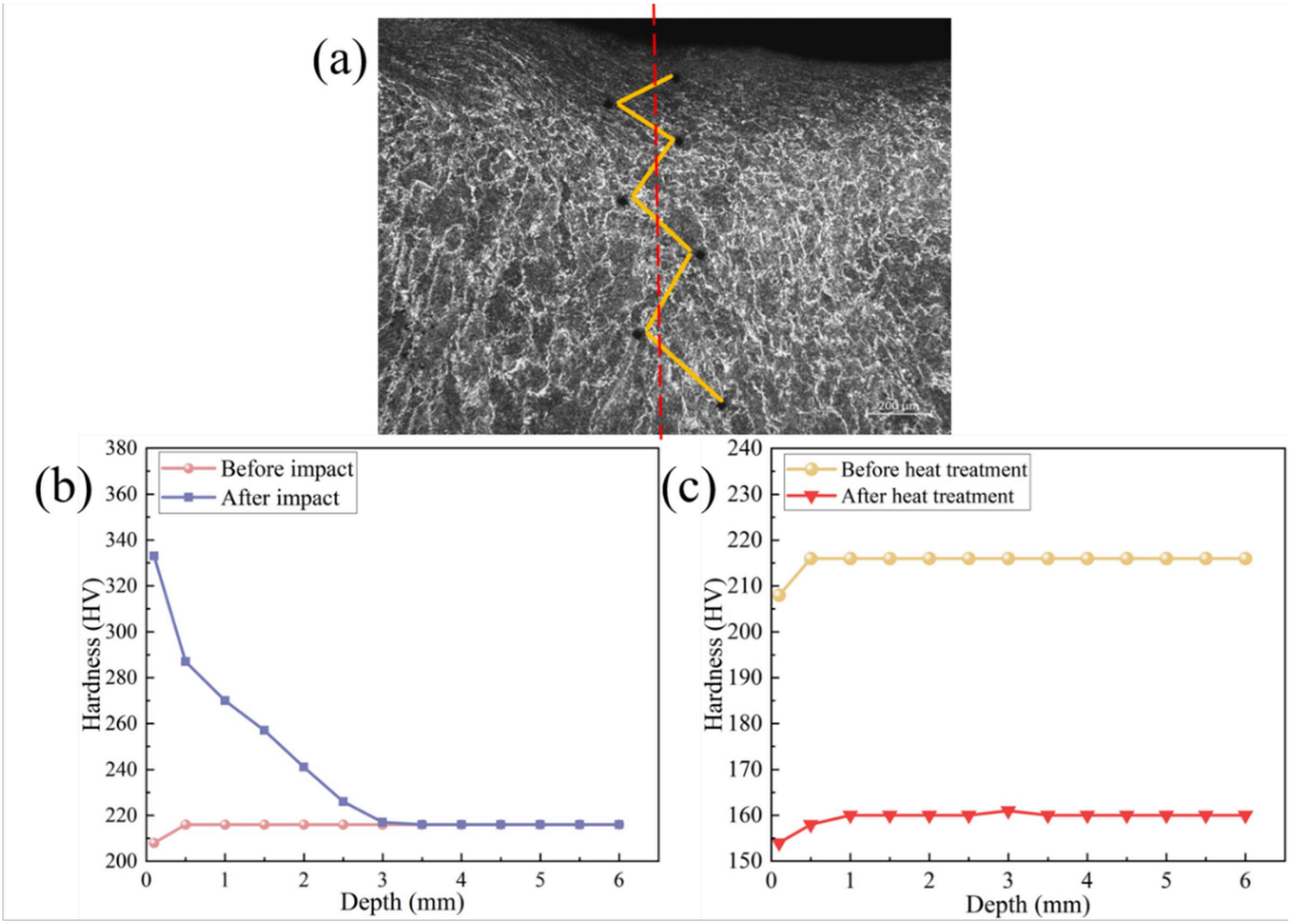


Figure 7

Hardness profile: (a) A diagram of measured points with Zigzag pattern; (b)Line chart of hardness before and after Ultrasonic impact;(c)Line chart of hardness before and after heat treatment